

Article

Analysis of Soil $\delta^{13}\text{C}$ and $\delta^{15}\text{N}$ Along Precipitation Gradient: Critical Insights into Tree–Grass Interactions and Soil C Sequestration in Savannas

Kebonye Dintwe ^{1,*}, Gregory S. Okin ², Frances O'Donnell ³, William P. Gilhooly III ⁴, Abinash Bhattachan ⁵, Mokganedi Tatlhego ⁶, Lixin Wang ⁴ and Paolo D'Odorico ⁷

¹ Department of Environmental Science, University of Botswana, Gaborone 00267, Botswana

² Department of Geography, University of California Los Angeles, Los Angeles, CA 90095, USA

³ Department of Civil and Environmental Engineering, Auburn University, Auburn, AL 36849, USA

⁴ Department of Earth and Environmental Sciences, Indiana University, Indianapolis, IN 46202, USA

⁵ Department of Earth and Environmental Sciences, California State University East Bay, Hayward, CA 94542, USA

⁶ Department of Environmental Science, Botswana International University of Science and Technology, Palapye 00267, Botswana

⁷ Department of Environmental Science, Policy, and Management, University of California, Berkeley, CA 94720, USA; paolododo@berkeley.edu

* Correspondence: dintwek@ub.ac.bw

Abstract

In situ observations of belowground tree–grass interactions are sparse in savanna ecosystems. In this study, we analyzed stable carbon and nitrogen isotopes ($\delta^{13}\text{C}$ and $\delta^{15}\text{N}$) in soils and plants from four study sites in an African savanna ecosystem along the Kalahari moisture gradient. The homogeneous soil texture, primarily sandy soils, is well-drained and nutrient-poor, influencing vegetation and water retention uniformly across the region. At each site, soil samples were collected from a 120 cm deep soil profile. We used a 2-endmember mass balance approach to calculate the relative contributions of C_3 and C_4 plants to SOC in the 120 m soil profile. The wettest site was dominated by trees, whereas the driest site was dominated by shrubs. The intermediates had the highest amount of grass biomass. Our results revealed that tree- and shrub-derived SOC was highest in the wettest and driest sites, respectively. The contribution of C_3 plants was 63.8% and 55.8%, in the wettest and driest sites, respectively, when integrating the 120 cm depth. Grass-derived SOC was highest (69.4%) in the middle of the precipitation gradient when integrating the 120 cm depth. The $\delta^{15}\text{N}$ values were highest in the middle of the precipitation gradient (10.7‰) and lowest in the wettest site (5.2‰). Our findings indicate that belowground tree–grass interactions and nitrogen cycling in savanna ecosystems are more complex than previously thought and do not conform to the traditional concept of the two-layer roots hypothesis. This lack of conformity could be attributed to several factors, including overlap in rooting depth and ecological drivers, such as wildfires and herbivory, which could stimulate production of belowground biomass. We used space-for-time substitution to leverage the region's steep north–south precipitation gradient and homogeneous soil texture. Our results indicated that trees and shrubs would become an important SOC source in the two extreme sites of the transect, while grass would become an important SOC source in the middle of the precipitation gradient.

Keywords: savannas; soil organic carbon; total nitrogen; tree–grass interaction; carbon sequestration; climate change



Academic Editors: Paul Aplin, Elias Symeonakis and Moses Azong Cho

Received: 1 September 2025

Revised: 28 September 2025

Accepted: 1 October 2025

Published: 27 November 2025

Citation: Dintwe, K.; Okin, G.S.; O'Donnell, F.; Gilhooly, W.P., III; Bhattachan, A.; Tatlhego, M.; Wang, L.; D'Odorico, P. Analysis of Soil $\delta^{13}\text{C}$ and $\delta^{15}\text{N}$ Along Precipitation Gradient: Critical Insights into Tree–Grass Interactions and Soil C Sequestration in Savannas. *Land* **2025**, *14*, 2328. <https://doi.org/10.3390/land14122328>

Copyright: © 2025 by the authors. Licensee MDPI, Basel, Switzerland. This article is an open access article distributed under the terms and conditions of the Creative Commons Attribution (CC BY) license (<https://creativecommons.org/licenses/by/4.0/>).

1. Introduction

Savannas are characterized by coexistence of trees and grasses and cover about 23–33 million km², or about one-fifth, of the Earth's land surface [1–3]. They are found in the latitude band ~15–30° in the south and north of the equator, where the mean annual precipitation (MAP) ranges between 100 and 1500 mm yr⁻¹ [4,5]. Equilibrium theory proposes that competition for water between woody and grass plants is a key determinant of the composition of the two life forms (trees and grasses). The theory suggests that competition is excluded based on the assumption that trees and grasses have ecological niches [6–10]. Because soil moisture varies with depth, grasses are efficient at exploiting moisture in the topsoil, whereas trees have exclusive access to water in the subsoil.

Savannas are an important component of drylands and global carbon stock, containing 15–20% of global soil organic carbon (SOC) [11–15]. SOC stocks in savannas are facing potential challenges from anthropogenic climate change and associated extreme weather events such as drought and windstorms [16–19]. Global climate models predict that savannas, particularly in southern Africa, would experience a 15% decrease in mean annual precipitation (MAP) and a 1.5 to 4 °C increase in mean annual temperature (MAT) by the end of the 21st century [18–20]. Regionally, the models predict an increase in the frequency and magnitude of associated extreme weather events such as wildfires, lightning, and droughts in Southern Africa. At the local scale, Batisani and Yarnal [21] observed a trend where rainfall decreases over time for the past decade in Botswana Kalahari (i.e., the area inside Botswana underlain by Kalahari Sands).

Dintwe and Okin [22] estimated that global savannas will lose ~28.4 Tg C y⁻¹ and 64.1 Tg C yr⁻¹ under Representative Concentration Pathway 2.6 (RCP2.6) and RCP8.5, respectively. Furthermore, they cautioned that the rapid loss of C from savanna soils through soil respiration could accelerate global warming and strengthen positive feedback mechanisms between climate change and processes controlling SOC. Vegetation models predict that plant productivity and SOC stocks in savannas, particularly in Africa, would decrease due to a decrease in precipitation [23]. Few studies in the Kalahari and across the world indicate that a decrease in precipitation causes a decline in net primary productivity (NPP), which ultimately leads to a decline in soil C sequestration [22,24]. Zeng and Neelin [25] used the QTCM model and concluded that a decrease in precipitation could increase vegetation productivity in African savannas, and ultimately in SOC sequestration. In Australia savannas, [26] estimated total carbon stock to be 204 ton C ha⁻¹, with about 84% belowground, 16% aboveground, and SOC accounting for about 74% of the total carbon content. Grace, Post [27] used the SOCRATES terrestrial carbon model to estimate changes in SOC for the Australian continent between the years 1990 and 2100 in response to climate change. They found that under a high greenhouse gas emissions scenario, the Australian continent becomes a source of CO₂ with a net reduction of 6.4% (518 Mt) in topsoil carbon, when compared to no climate change. Similarly, ref. [28] projected a decline in SOC stocks over south-eastern Australia until ~2070 due to changes in temperatures and rainfall in the region. In South American savannas, the Cerrado stores a significant amount of SOC, estimated at over 13 gigatons in the top 1 m of the soil, with a vertical distribution pattern of 26% in the upper 0–30 cm layer, 38% in the 30–100 cm layer, and 36% in the 100–200 cm layer [29,30]. However, SOC in South America, particularly in Brazil, is expected to decrease due to the combined effects of climate change and agricultural expansion [31,32]. Wei, Shao [33] showed that at the global scale, climate and soil factors affected the decrease in SOC stocks. Precipitation, depending on its intensity and frequency, could have varying outcomes on vegetation productivity, and ultimately soil carbon sequestration and nutrient cycling. For instance, small increases in precipitation intensity may increase plant productivity by decreasing interception and evaporation [34]. Alter-

natively, a large increase in precipitation intensity and associated decrease in frequency may decrease plant productivity due to deep soil infiltration and lower soil moisture in surface layers [35,36]. Moreover, vegetation responds to short-term variation in precipitation through adjustments in plant physiology, whereas long-term variation is mediated by plant establishment, composition, and disturbance regimes [37,38]. However, it is still not clear how climate change, particularly precipitation, will affect soil C sequestration and nutrient cycling in savanna ecosystems. With these contradictory analyses, it is clear that more work needs to be done in order to assess and understand the potential impacts of climate change on SOC balance in the savanna [39–41].

The objective of this study is to determine the impact of climate change on soil C sequestration in savanna ecosystems. We used stable C and N isotopes ($\delta^{13}\text{C}$ and $\delta^{15}\text{N}$) to assess the long-term impacts of climate on C and N pools in the soil profile in a savanna ecosystem along a steep precipitation gradient (180–540 mm yr⁻¹). Stable isotopes of nitrogen ($\delta^{15}\text{N}$) are used to evaluate whether the abundant Mimosaceae in the Kalahari and other plants contribute nitrogen (N) to the system. Nitrogen is an essential plant nutrient and one of the limiting nutrients in savanna ecosystems [42–44]. Because plants are the major terrestrial producers and sources of soil organic C (SOC), soil carbon stocks record and reflect the long-term interactions between trees and grasses [45–47]. $\delta^{13}\text{C}$ values of SOC relate to the ¹³C of plants residues mainly through root turnover [48]. Thus, the soil profile $\delta^{13}\text{C}$ may be used as a proxy to identify sources of SOC and thus infer the belowground tree–grass relationships. This analysis of $\delta^{13}\text{C}$ along a precipitation gradient elucidates both belowground interactions between plant functional types as well as the effect of this interaction under different precipitation regimes. Based on the previous work in the Kalahari [48–50], we hypothesized that the drier sites of the Kalahari will have relatively low soil C input from trees, shrubs and grasses, and inversely wetter sites will have relatively more soil C input from trees, shrubs and grasses. However, it is important to point out that this study differs from earlier studies in the sense that more intensive work (e.g., more sites and deeper soil profiles) was done in soil sampling and analysis.

2. Materials and Methods

2.1. Study Site Description

The study was conducted in the Kalahari Transect (KT) in southern Africa (Figure 1). The Kalahari basin covers an area of about 2.5 million km² between 12–29° S and 14–28° E, along a steep north–south precipitation gradient [16,51,52]. While the mean annual precipitation (MAP) in the north could be as high as 1200 mm, the south receives as little as 150 mm. The Botswana Kalahari stretches 1000 km in the north–south direction across the western part of the country along a rainfall gradient ranging from 650 mm yr⁻¹ in the north to 180 mm yr⁻¹ in the south [49]. Potential evapotranspiration rates vary from 1000 mm yr⁻¹ in the north to >2000 mm yr⁻¹ in the south [53].

Soils in the Kalahari are deep homogeneous aeolian sand deposits reaching 100–200 m depth in the center of the basin [52,54,55]. The soils in the Kalahari are slightly acidic, about ~95% sand, and poor in organic carbon and total nitrogen content [14,22,56]. Throughout much of the Kalahari, groundwater is deep (>20 m) [57], meaning that plants rely almost exclusively on precipitation (Table 1).

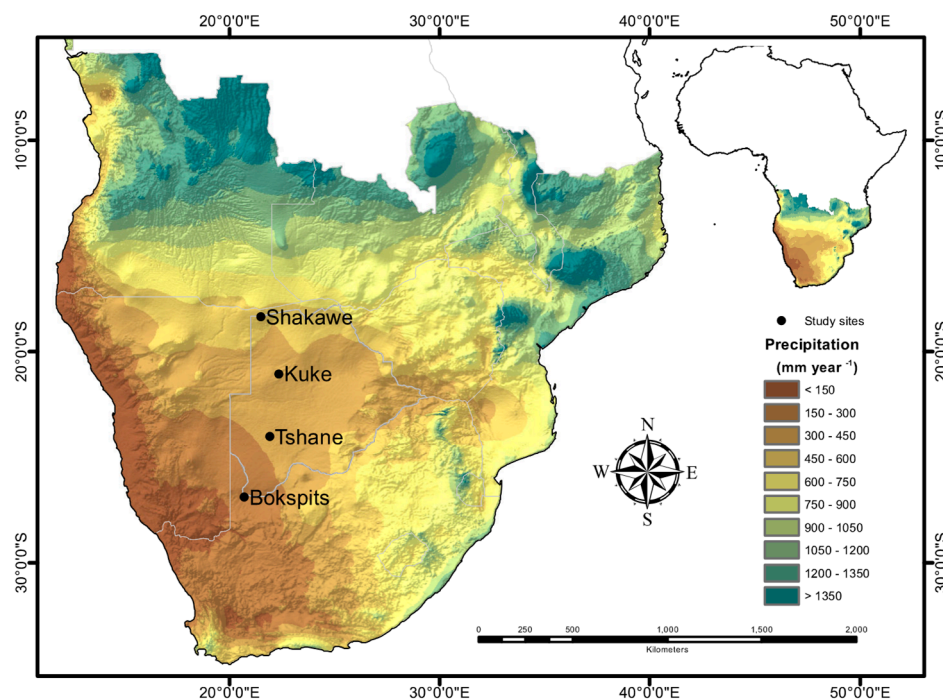


Figure 1. Mean annual precipitation in southern Africa. The southern part receives less rainfall, while the equatorial region in the north receives the highest amount of precipitation.

Table 1. Geographic coordinates, climate parameters, soil, and vegetation characteristics of the study sites. The $\delta^{13}\text{C}$ values for trees and grasses are obtained from [48,58], whereas tree $\delta^{15}\text{N}$ values are obtained from [48,59].

Site Feature	Bokspits	Tshane	Kuke	Shakawe
Geographic Coordinates	26°53'39" S 20°41'54" E	24°01'01" S 21°52'08" E	20°58'36" S 22°28'48" E	18°21'51" S 21°50'31" E
Mean Annual Precipitation (mm)	180	360	440	540
Mean Min Temp (°C)	2.1	3.9	4.4	5.8
Mean Max Temp (°C)	34.3	33.5	33.4	33.7
Soil pH	6.7	5.6	5.9	5.4
Organic Carbon (g m^{-2})	1397.0	2506.0	2136.0	1982.0
Woody biomass (g m^{-2})	0.15	0.31	0.40	0.52
Nitrogen (g m^{-2})	78.6	151.0	135.0	107.0
C ₃ Foliar $\delta^{13}\text{C}_{\text{VPDB}}$ (‰)	−23.2	−25.9	−25.9	−26.7
C ₄ Foliar $\delta^{13}\text{C}_{\text{VPDB}}$ (‰)	−14.0	−14.2	−13.8	−13.4
C ₃ foliar $\delta^{15}\text{N}_{\text{atm}}$ (‰)	7.40	6.82	7.27	3.50

The vegetation structure (e.g., diversity and canopy cover) in the Kalahari is strongly tied to the north–south precipitation gradient [55,60]. Shrubs and trees in the dry portions of the Kalahari contribute significantly to the patterning of soil resources, whereas in wet portions, only trees contribute to the patterning of soil resources [61]. The dominant plant species in the wettest part of Kalahari (north) are nutrient-poor broad-leaf Combretaceae and Caesalpinaeae, whilst in the driest (south) part are C₄ grasses, with sparsely distributed nutrient-rich fine-leaf Mimosaceae [49,54,55,60,62–64]. Among the Poaceae, the Aristidae (Aristida and *Stipagrostis* spp.) dominate the arid south, the Panicoidae in the semi-arid center, while the Andropogonae dominate in the mesic north [55].

The KT was identified by the IGBP (International Geosphere-Biosphere Programme) as one of the ‘mega-transects’ for global change studies [55]. With a remarkably steep precipitation gradient, lack of relief, and homogeneous soil texture, the KT provides an

ideal setting to study the impact of climate on carbon dynamics with minimal confounding variables.

2.2. Sample Design

Four study sites were selected along the Kalahari transect (KT) along the north–south precipitation gradient (Figure 1). Three 20 m × 20 m plots were established at each site, with each plot resulting in 400, 1 m × 1 m quadrats. Vegetation was characterized on each plot before removal, see [62]. The cleared plots were gridded into 1 × 1 m quadrats. Eighty (80) of the 1 m × 1 m quadrats were randomly selected and sampled in the center with a 4-inch (~10 cm) diameter sand auger (AMS Inc, Pittsburgh, PA, USA) at four depths. The auger was inserted in the center of each quadrat until its tip was at 10, 30, 70, and 120 cm depth [65]. Upon reaching each of these depths, the auger was removed, and a mixed sample from the auger was extracted. Thus, the average depth for the samples was approximately 5, 20, 50, and 95 cm. About 50 g of soil was taken at each depth and stored in a labeled zip-lock bag. The bags were left open for a week to air dry before being shipped to the USA for laboratory analysis.

2.3. Laboratory Analysis

Each labeled bag of soil was sieved, thoroughly mixed, and sub-sampled using a riffle sampler. Soil grain size distribution was measured in a subset of soil samples following a method outlined by [66,67]. For this, approximately 0.5 cm³ of sample was boiled in DI water and pretreated with about 50 mL of 30% H₂O₂ to remove organic matter, 10 mL of 1 N HCl was used to remove carbonates, and 10 mL of 1 N NaOH was used to remove biogenic silica. Grain size was measured using the Malvern Mastersizer 2000 G (Malvern Panalytical, Malvern, Worcestershire, United Kingdom) large-volume sample dispersion unit. To verify the equipment's accuracy, repeatability and stability, a tuff standard (TS2) with a known distribution between 1.0 μm and 16 μm (mean = 4.53 μm ± 0.07 μm, *n* = 2998) was run regularly. The TS2 was run every few samples and once at the end for a final assessment. The results were reported as volume percent and divided into sand (74.00–2000 μm), silt (3.90–73.99 μm) and clay (0.02–3.89 μm) [66].

Subsamples of about 4–5 cm³ were ground into a powder using a ball mill for three minutes at 3450 rpm (Cianflone Scientific Instruments Corporation, Pittsburgh, PA, USA). Thirty-three samples for each depth at 10 and 30 cm, and fifteen samples each depth at 70 and 120 cm were randomly selected for each site for δ¹³C and δ¹⁵N analysis. A small portion, approximately 190 mg, of the ground, homogenized soil was placed into a 9 × 10 mm tin capsule (Costech Analytical, Valencia, CA, USA). Before being sealed, the soils in the open silver capsules were fumigated in an atmosphere created by a beaker of concentrated HCl placed in a bell jar for 24 h in order to remove carbonates [68]. After being sealed, the sample was combusted on an Elemental Combustion System (Costech Analytical, Valencia, CA, USA) interfaced by continuous gas flow ConFlo IV (Thermo Scientific, Bremen, Germany) to a stable isotope ratio mass spectrometer (Delta V Plus, Thermo Scientific, Bremen, Germany). SOC and total nitrogen (TN) results are from [14]. Tree δ¹⁵N values are obtained from [48,59], whereas δ¹³C values for trees and grasses are obtained from [48,58].

The δ¹³C in the soil samples was normalized to the international standards USGS-40 (L-glutamic acid) and Buffalo River Sediments (SRM 2704), while ammonium sulfate (IAEA-N-1) was used as the standard for δ¹⁵N [69–76]. The isotope ratios were calculated using Equation (1), where *R* was the element measured, *x* was the heavier isotope and *y* was the lighter isotope of the element measured [65,70,72,77–80].

$$\delta^x R\text{‰} = \left(\frac{(xR/yR)_{\text{sample}}}{(xR/yR)_{\text{standard}}} - 1 \right) * 10^3 = \frac{(R_{\text{sample}} - R_{\text{standard}})}{R_{\text{standard}}} * 10^3 \quad (1)$$

By convention, the $\delta^{13}\text{C}$ and $\delta^{15}\text{N}$ were corrected and reported as parts per thousand (per mil) relative to that for Vienna Pee Dee Belemnite (VPDB) and atmospheric N_2 , respectively [71,76,81]. Reproducibility of these measurements was approximately $\pm 0.2\text{‰}$.

2.4. Statistical Analysis

Descriptive statistics such as mean, median, and standard deviation were used to analyze the measured variables and to indicate the degree of overall variation. Analysis of variance (ANOVA) was used to test for differences between samples, depth, and sites. Fisher's least significant difference (LSD) method was used to distinguish differences following the ANOVA test. We further used linear and multiple regression techniques to evaluate the relationship between isotope values and climate variables.

We calculated the difference between C_3 foliar $\delta^{15}\text{N}$ and the potential sources of plant N, which are soil and the atmosphere. The difference ($\Delta^{15}\text{N}$) was used to identify the dominant source of plant N as well as to estimate the isotopic composition of plant available N [82–85]. By definition, the $\delta^{15}\text{N}$ of the atmospheric N_2 is 0‰ , whereas that of the soil is usually greater than 0‰ , especially in drier environments [86]. Therefore, $\delta^{15}\text{N}$ of N-fixing plants should be very close to 0‰ ($\pm 2\text{‰}$), with slight modification by diffusion fractionation and the isotope effect associated with N fixation [87,88]. At present, there is no easy and straightforward technique for isolating and analyzing $\delta^{15}\text{N}$ in the soil pools that are available for plant uptake [89].

To estimate the proportion of SOC from trees and grasses, we assumed that SOC was made up of the sum of the fractions (F_i) contributed from the sources (δ_i), where the sources were C_3 and C_4 plant species (Equation (2)).

$$\delta^{13}\text{C}_{\text{soil}} = \sum_{i=1}^n F_i \delta_i \quad (2)$$

Assuming the soil is a mixture of organic matter from C_3 and C_4 plants, we used a simple 2-endmember mass balance equation to calculate the relative contributions of C_3 and C_4 plants to SOC in the 120 m soil profile (Equation (3)):

$$C_x(\%) = \frac{\delta^{13}\text{C}_{\text{soc}} - \delta^{13}\text{C}_y}{\delta^{13}\text{C}_x - \delta^{13}\text{C}_y} \times 100 \quad (3)$$

where the $\delta^{13}\text{C}$ of SOC ($\delta^{13}\text{C}_{\text{soc}}$) comprises end-members with unique $\delta^{13}\text{C}$ values ($\delta^{13}\text{C}_x$ and $\delta^{13}\text{C}_y$) [90,91]. Values of $\delta^{13}\text{C}-\text{C}_3$ and $\delta^{13}\text{C}-\text{C}_4$ derived from the literature for measurements made in areas of the Kalahari with MAP comparable to our locations were used for these calculations [48,58] (Table 1). Studies in the Kalahari show that dominant plant species belong to C_3 and C_4 , and that CAM plants are almost absent [62,92], suggesting that CAM plants are not a significant SOC source.

Because the amount of SOC declined with depth (e.g., Dintwe, Okin [14], an exponential decay function, $C = C_0 e^{-kz}$, was used to estimate total C contribution from trees and grasses in the soil profile, where C (concentration at depth) and C_0 (surface concentration) were in units of g m^{-3} . The parameters of the equation, C_0 and k (m^{-1}) were determined by least squares fitting of measured concentrations with depth, z . The total C contribution was calculated by taking the integral of the equation from 0 to 1 m:

$$\int C_0 e^{-kz} dz = -C_0 e^{-kz} \Big|_0^1 \text{m} \quad (4)$$

We calculated Z_{50} and Z_{95} of the soil profile, which are the depths above which 50% and 95% of the total C contribution occurs, respectively. Furthermore, we calculate the e-folding depth ($1/k$). The e-folding depth is the depth at which C contribution decreases to $1/e$ of the surface value.

3. Results

3.1. Soil Texture

The soils in the Kalahari contained more than 90% sand at all sites and depths except in Bokspits at 120 cm, where sand content was 88% (Table 2). Shakawe had the highest sand content, containing more than 98% at all depths. Clay content was highest in Tshane, followed by Kuke, Bokspits, and Shakawe, respectively. Silt content increased with soil depth in all the sites except in Shakawe.

Table 2. Soil texture in the Kalahari Transect. Kalahari soils contain more than 90% sand.

Site (MAP)	Depth (cm)	Clay	Silt	Sand
		(% Composition)		
Bokspits (180 mm)	10	0.55	3.10	96.34
	30	0.67	3.56	95.76
	70	0.81	4.36	94.82
	120	1.30	10.36	88.32
	0–120	0.97	6.62	92.39
Tshane (350 mm)	10	1.54	5.01	93.43
	30	1.13	6.30	92.55
	70	1.52	7.76	90.70
	120	1.58	8.17	90.22
	0–120	1.48	7.46	91.04
Kuke (440 mm)	10	1.15	3.44	95.40
	30	0.87	3.88	95.23
	70	1.05	4.56	94.38
	120	1.00	4.59	94.39
	0–120	1.01	4.37	94.61
Shakawe (540 mm)	10	0.00	1.02	98.98
	30	0.00	0.83	99.16
	70	0.00	0.00	99.99
	120	0.00	1.21	98.79
	0–120	0.00	0.73	99.27

The mean soil $\delta^{13}\text{C}$ values ranged between -22.7‰ and -17.3‰ (Figure 2). The highest $\delta^{13}\text{C}$ value at 10 cm was recorded at Tshane (-18.9‰), followed by Bokspits with -19.0‰ . The lowest $\delta^{13}\text{C}$ value at 10 cm depth (-22.2‰) was recorded at Shakawe. Similarly, Tshane had the highest depth-weighted $\delta^{13}\text{C}$ average for the soil profile, followed by Bokspits, Kuke and Shakawe.

The highest $\delta^{13}\text{C}$ values occurred at 30 cm in all the sites, and the second-highest values were found at 10 cm. Soil organic carbon was highest at 10 cm in all the sites, followed by the 10–30 cm layer. Shakawe (wettest) had the lowest mean $\delta^{13}\text{C}$ values, and Tshane had the highest values. In general, soil $\delta^{13}\text{C}$ values decreased with MAP, consistent with the pattern observed in other studies around the world [43,56,93–98]. The mean SOC was highest in Tshane and lowest in Bokspits (driest). There was a relatively strong correlation between mean $\delta^{13}\text{C}$ and clay content in the soil profile along the KT ($r^2 = 0.63$, p -value < 0.001).

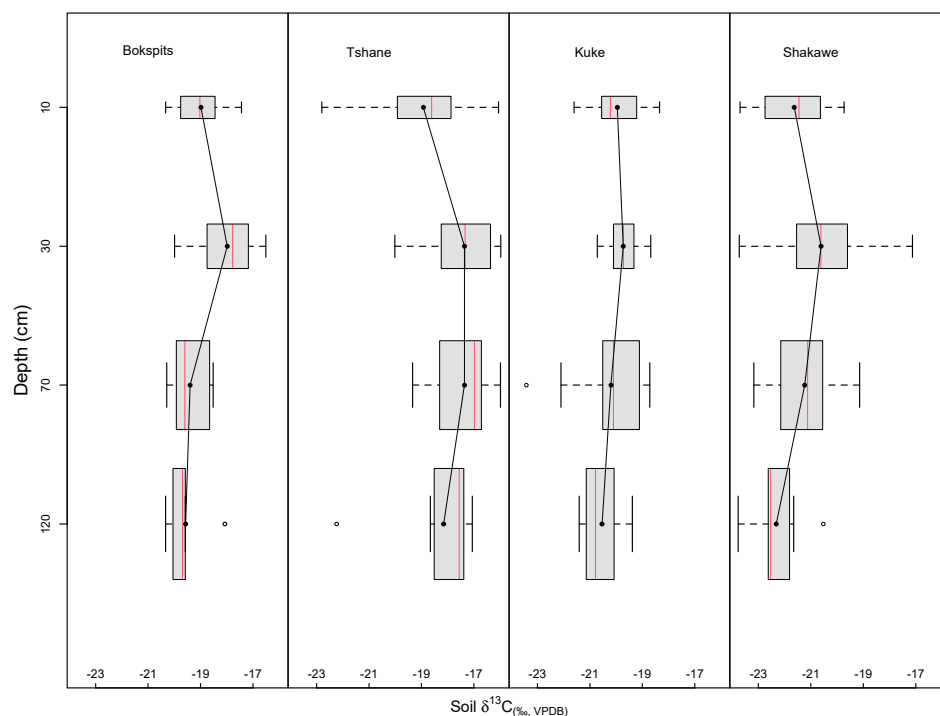


Figure 2. Soil $\delta^{13}\text{C}$ values along the Kalahari moisture gradient. The wettest site had the lowest soil $\delta^{13}\text{C}$ values. Soil $\delta^{13}\text{C}$ values were highest at 30 cm depth in all the sites.

3.2. SOC Input from Trees and Grasses

The percentage contribution of trees (C_3) to SOC, as estimated from $\delta^{13}\text{C}_{\text{soc}}$, was highest in Shakawe (wettest), and lowest in Tshane (Table S1). The highest contribution of C_3 -derived organic matter to the SOC pool was recorded at 10 cm in all the sites. The C_3 contribution at 70 cm was higher than at 30 cm in all the sites, except in Tshane, where the C_3 contribution at 30 cm and 70 cm were statistically indistinguishable. The depth-weighted mean tree SOC contribution in Shakawe was about 64% (0.66 mg C g^{-1}), while SOC in Tshane was approximately 31% (0.48 mg C g^{-1}) (Figure 2). Overall, the contribution of C_3 to SOC increased with MAP, with Bokspits recording 769.4 g C m^{-2} , whereas Shakawe recorded $1288.1 \text{ g C m}^{-2}$ (Figure 3).

The intermediate sites had higher grass (C_4) SOC contribution than the wettest and driest sites (Figure 2). The highest C_4 contribution was at 30 cm in all the sites. Bokspits has the lowest absolute C_4 contribution, while Tshane had the highest absolute contribution, 648 g C m^{-2} and $1721.0 \text{ g C m}^{-2}$, respectively (Figure 3). Grass carbon contribution had a non-linear relationship with MAP. The contribution increased with MAP, reached a maximum in Tshane, and then decreased with an increasing MAP. In contrast, tree carbon contribution increased with increasing MAP. The SOC contribution from C_3 plants was higher than the C_4 input at 10 cm, except in Tshane, where C_4 had a higher contribution. The C_4 contribution was higher than the C_3 contribution at 30 cm in the intermediate sites (Tshane and Kuke), lower than the C_3 contribution in the two extreme sites (Bokspits and Shakawe). The e-folding depth for C_3 -derived carbon was lowest in Shakawe and highest in Bokspits, 0.6 m and 2.1 m, respectively (Figure 3).

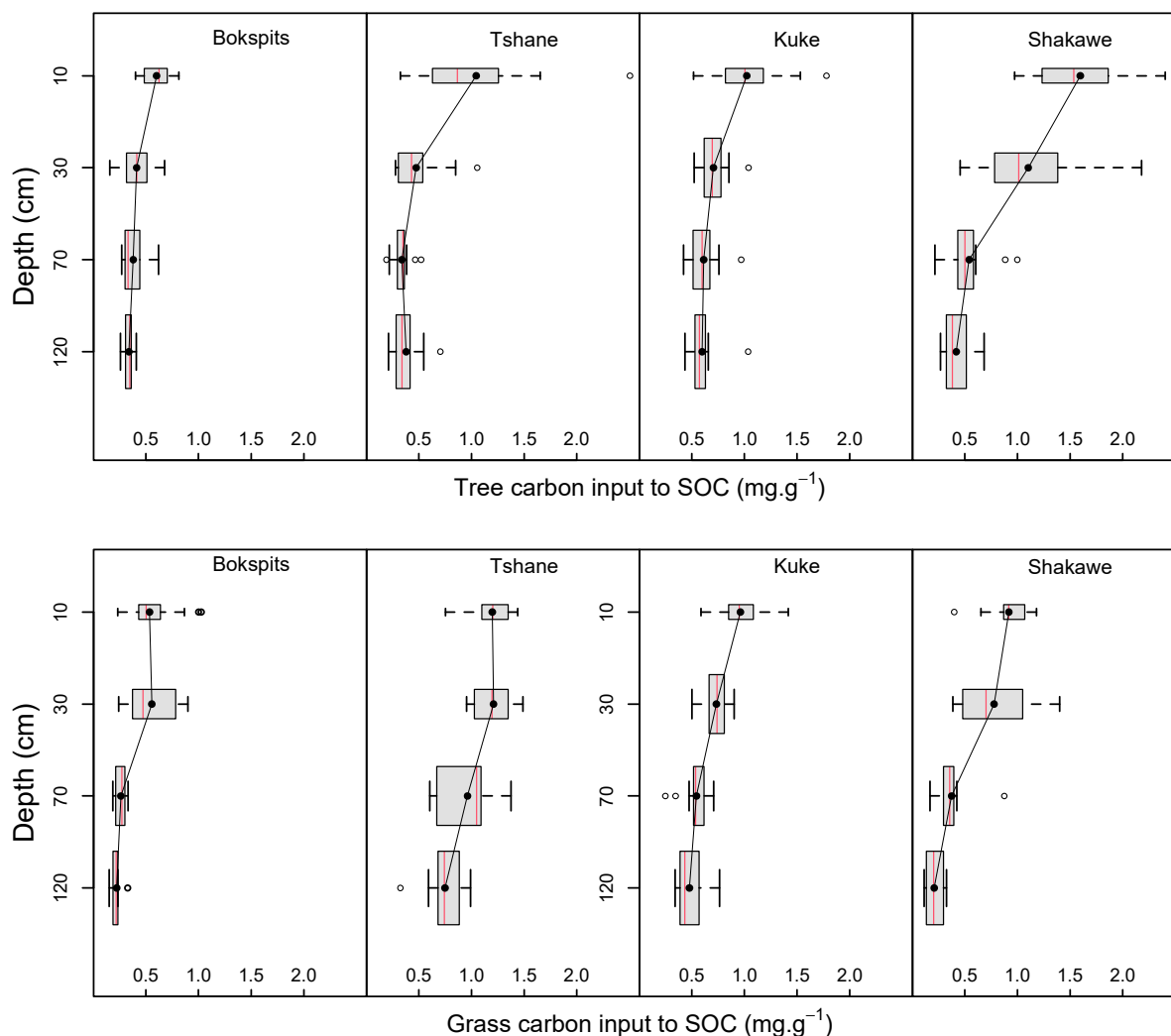


Figure 3. Tree–grass soil C input along the Kalahari moisture gradient. In the wettest site, trees contributed the highest to soil carbon content, whereas grasses contributed the highest in the intermediate site.

3.3. Soil $\delta^{15}\text{N}$

The mean soil $\delta^{15}\text{N}$ values ranged between 1.6‰ and 10.7‰ (Figure 4). The two intermediate sites, Tshane and Kuke, had the highest $\delta^{15}\text{N}$ values of 10.7‰ and 8.6‰, respectively, at 10 cm depth. The two extreme sites (driest and wettest), Bokspits and Shakawe, had 7.4‰ and 5.2‰, respectively. Similarly, the intermediate sites had the highest depth-weighted mean $\delta^{15}\text{N}$ values, and the two extreme sites had the lowest depth-weighted mean $\delta^{15}\text{N}$ values. Although the mean TN in Bokspits was the same as in Shakawe, the mean $\delta^{15}\text{N}$ in Bokspits was twice as high as in Shakawe (Figure 4). Shakawe had the overall lowest $\delta^{15}\text{N}$ values in the soil profile compared to other sites.

The difference between plant and soil $\delta^{15}\text{N}$ was highest in Tshane (the second driest site) and lowest in Kuke. The difference between plant and atmospheric $\delta^{15}\text{N}$ was highest in the driest site and lowest in the wettest site. The difference between foliar and atmospheric $\delta^{15}\text{N}$ was higher than the difference between foliar and soil $\delta^{15}\text{N}$ in all the sites.

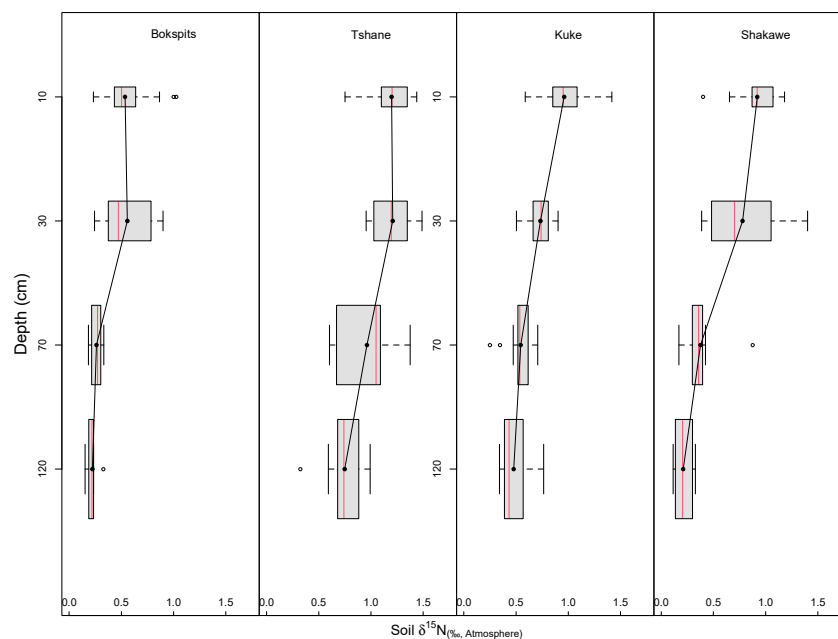


Figure 4. The driest site had the lowest soil $\delta^{15}\text{N}$ values compared to other sites, at 10 cm. At 30 cm, the wettest site had the highest soil $\delta^{15}\text{N}$ values.

4. Discussion

4.1. Soil Texture

The soil texture results indicate that Kalahari soils contain more than 90% sand (90% quartz), which is consistent with other research findings [52,99,100]. The lack of relationship between grain particle size and precipitation could be attributed to the fact that Kalahari sand deposits are a result of aeolian processes [52], and are independent of precipitation and biological weathering. Although precipitation decreased in the north–south direction, there was no relationship between soil texture and the north–south precipitation gradient. No trends were observed between soil texture and depth, which suggests that biological weathering does not play any significant role in the soil texture of the Kalahari. Furthermore, there was no correlation between soil texture and vegetation structure (woody biomass), which again suggests that vegetation structure, particularly root activity, does not influence soil texture.

4.2. Soil Profile $\delta^{13}\text{C}$ and Tree–Grass Belowground Interaction

In general, soil $\delta^{13}\text{C}$ values decreased in the south–north direction, following an increase in the south–north MAP, a pattern observed in other studies around the world [43,66,94–99]. The relationship between trees and precipitation suggests that as MAP increases, trees become more dominant and consequently, an important source of SOC, consistent with the global-scale distribution of woodlands [1,2,101].

Soil $\delta^{13}\text{C}$ values and estimated tree vs. grass C inputs show a distinct and consistent pattern in the soil profile in all the sites, with $\delta^{13}\text{C}$ increasing to 30 cm (or 70 cm, in the case of Tshane) and then decreasing below the 30 cm depth (Figure 2). This pattern is inconsistent with what is expected purely from Rayleigh distillation, e.g., [102], in which enrichment occurs as microbial processes break down SOM during downward translocation in the soil, resulting in a monotonic increase in $\delta^{13}\text{C}$ with depth. This is not surprising, as Wynn, Bird [103] showed that though the Rayleigh distillation model may work for heavy-textured soils, this model is inappropriate for sandy soils like those in the Kalahari. Indeed, ref. [46] have suggested that changes in $\delta^{13}\text{C}$ are not, in fact, due to Rayleigh fractionation, leaving the validity of this model in question.

Wang, Okin [96] measured surface spatial variations of $\delta^{13}\text{C}$ in the Kalahari. The reported $\delta^{13}\text{C}$ values from their sites were highly consistent with the spatial distribution of trees and grasses, thus suggesting that the isotopic compositions in the soil are meaningful representations of the source of carbon. This pattern gives us confidence that the differences observed with soil depth in the present study are meaningful. Thus, we conclude that the relatively depleted $\delta^{13}\text{C}$ values in the top 10 cm and below 30 cm suggest the importance of tree input at these depths; whereas the relatively higher $\delta^{13}\text{C}$ values in the 30 cm layer observed at all sites suggest the importance of grass input (Figure 2). Our findings are consistent with those of [104], who used stable C isotope analysis in African humid savannas and found that fine roots from trees peaked at 10 cm and below 30 cm, while fine roots from grasses peaked at 20 cm. We therefore believe that the best explanation for the observed peaked $\delta^{13}\text{C}$ pattern (i.e., enrichment in ^{13}C at 30 cm, or 30 cm and 70 cm in the case of Tshane, compared to the other soil layers) is that the measured values represent the carbon emplaced by plant roots at those depths. In mesic and semiarid savanna ecosystems in Australia and southern Africa, stable C isotope analysis revealed that tree and grass fine roots were concentrated in the top 20 cm of the soil [105,106].

In the Sonoran desert, Nilsen, Sharifi [107] found that the tree *Prosopis* developed two distinct root systems, whereby root mats occurred at 10 cm and below 60 cm. Kambatuku, Cramer [108] investigated belowground interactions between trees and grasses, and found that grasses exclusively exploited the 15 cm layer, whereas trees exclusively exploited the deeper subsoil layer at 35 cm. Although the [108] experiment was under a controlled environment, its findings highlight the importance of niche separation between trees and grasses in a savanna ecosystem.

4.3. Soil Profile $\delta^{13}\text{C}$ and Precipitation Gradient

The contribution of C_3 plants to SOC was consistent with vegetation structure in the Kalahari, where tree cover and height increased with MAP [4,55,60] (Table 1). Studies from other parts of the world have shown a similar pattern, where woody contribution increased with MAP [43,48,93]. The e-folding depth and Z_{95} values for SOC from trees were lowest in Shakawe (Table 3), suggesting that trees in the area could be shallow-rooted. These results are consistent with the ones from both [100,109] studies for the same sites, where they found that 90% of tree root biomass was in the top 75 cm of the soil profile. It is important to reiterate that Kalahari sands have a homogeneous texture and, as a result, would have a uniform impact on $\delta^{13}\text{C}$ values. Therefore, variations in $\delta^{13}\text{C}$ values would be attributed to vegetation structure, which in turn is controlled by precipitation.

Table 3. Organic C contribution from trees and grasses. Organic C contribution from trees was highest in the wettest site and lowest in the driest site. The e-folding ($1/k$) is the depth at which SOC contribution decreases to $1/e$ of the surface value, whereas Z_{50} and Z_{95} refer to 50% and 95% of tree-derived SOC in the soil profile.

Site	Trees					Grasses		
	C_o (g m^{-3})	Tree Input (g m^{-2})	k (m)	e-Folding Depth (m)	Z_{50} (m)	Z_{95} (m)	C_o (g m^{-3})	Grass Input (g m^{-2})
Bokspits (180 mm)	965.5	769.4	0.5	2.1	1.5	6.3	881.0	648.0
Tshane (350 mm)	1216.7	808.4	0.9	1.1	0.8	3.4	2084.4	1721.0
Kuke (440 mm)	1423.2	1121.9	0.5	2.0	1.4	6.0	1470.3	1073.5
Shakawe (540 mm)	2729.5	1288.1	1.8	0.6	0.4	1.7	1583.9	830.6

The contribution of C_4 to SOC increased from Bokspits, reached a maximum in Tshane, and decreased with an increasing MAP. Our results are consistent with Scanlon, Albertson [110], who showed a non-linear relationship between aboveground grass biomass and MAP, and explained that grass cover peaks at the location with approximately 450 mm MAP. Soil $\delta^{13}C$ values indicated that the contribution of grass to SOM increases with MAP, reaching a maximum in Tshane, and decreasing at the wetter sites. At these intermediate sites, we speculate that lower overall precipitation (than in the north) reduces the growth of trees, thus allowing water to penetrate deeper into the soil to reach the intermediate-depth grass roots. The result of this would be production of more grass root biomass, which translates into high C sequestration. Furthermore, previous studies in the Kalahari indicated a peak in surface SOC and herbaceous cover in the middle of the Kalahari transect [110–112]. In light of this pattern, we follow Scanlon, Albertson [110] assessment in suggesting that low grass cover and productivity in the drier portion of Kalahari could be attributed to low soil moisture, whereas in the wet portion, the low grass cover and productivity could be attributed to belowground competition from trees for water or aboveground competition for light. The intermediate sites appear to provide optimal conditions for grass productivity, and this is reflected by the grass contributions to SOC. Trees in the intermediate sites may facilitate grass growth through improved soil water availability related to hydraulic lift, or through a reduction in incoming solar radiation [113,114]. Furthermore, facilitation might also be a result of improvement in nutrient availability related to litter inputs from trees [115].

4.4. Soil Profile $\delta^{15}N$ Along Precipitation Gradient

Nitrogen is one of the factors limiting productivity in the Kalahari, and plants rely on soil N fixed by cyanobacteria [42,59]. Our results show that the difference between foliar and soil $\delta^{15}N$ was lower than the difference between foliar and atmospheric $\delta^{15}N$ (Table S2). Conversely, foliar $\delta^{15}N$ values were closer to soil $\delta^{15}N$ values than atmospheric values, suggesting that plants in the Kalahari obtain most of their N from the soil rather than through fixation, even in the drier sites where the main woody species are Fabaceae. Aranibar, Otter [59] suggested that plants in the wetter portion of the Kalahari, where Fabaceae are largely absent, could be fixing nitrogen based on their low foliar $\delta^{15}N$ values. We have found that soil $\delta^{15}N$ values are also the lowest in Shakawe, our wettest site. It is possible that the low foliar $\delta^{15}N$ values found by Aranibar, Otter [59] in the wetter portion of the Kalahari do not necessarily suggest plant N-fixation but rather reflect the source of N. In fact, the relatively low soil $\delta^{15}N$ in Shakawe could be due to higher soil moisture, which facilitates fixation of atmospheric N by soil microbes. The rate of N fixation by microbes could be higher in the wetter portions of the Kalahari, and lower in the drier portions. The relatively high N-fixation by soil microbes in the wettest portion of the Kalahari could cause soil $\delta^{15}N$ to be closer to that of the atmosphere, compared to the drier portion of the Kalahari. A recent study [14] found that the C-to-N ratios of fine roots of Fabaceae in the Kalahari were not significantly lower (higher N) than those of other species/families, which suggested that Fabaceae were not fixing N_2 .

Thus, it is likely that C_3 and C_4 plants in the drier parts of the Kalahari have evolved under low soil N, and have developed adaptation mechanisms to access the limited soil N. Priyadarshini, Prins [116] suggested that grasses, which usually exhibit N limitation, benefit from N redirected by trees. Furthermore, the structure of the Kalahari soils, which are characterized by low quantities of clay and humus colloids (Table 2), low cation exchange capacities, and high porosity and permeability, could potentially enhance N leaching and redirection, leading to a relatively homogenous distribution of $\delta^{15}N$ in the soil, thus making N available to non-N-fixing plants [116].

4.5. Potential Impacts of Climate Change on C Cycling

Future climate change is expected to significantly alter the precipitation totals, increase warming by the end of this century, and lead to extreme weather events [18–20,117]. Anthropogenic climate change may alter vegetation composition in dryland ecosystems, particularly savannas [118–120]. Because vegetation is the primary source of SOC, changes in vegetation structure will have a direct impact on SOC stocks. In this study, our analysis indicated that SOC input from trees increases with MAP, which is consistent with results from our previous studies where we found low SOC quantities in drier sites of the Kalahari and higher SOC content in the wetter parts Dintwe, Okin [14]. Similarly, studies from other parts of the world indicated that soil C derived from woody plants increases as precipitation increases [43,93].

Because the Kalahari basin is characterized by homogeneous sandy soil and the north–south precipitation gradient, we used a space-for-time substitution approach to assess future climate conditions in soil C stocks. Our results showed that a decrease in precipitation would cause a decrease in the overall soil C sequestration, whereas an increase in precipitation would increase soil C. Dintwe and Okin [22] showed that a decrease in precipitation causes a decrease in net primary productivity (NPP), whereas an increase in temperature results in the overall decrease in NPP and soil respiration. Furthermore, their study revealed that the effect of increased temperature in SOC was more pronounced in the driest and wettest parts of the Kalahari, whereas the effect of precipitation (decrease) was more pronounced in the intermediate sites.

Some parts of the Southern African savannas may become woodier due to increasing CO₂ concentration and thicketization [120,121]. Under these perceived circumstances, C₃ contribution to SOC input will become important, as in the case of Bokspits (driest part), where shrubs play an important role in SOC input. Using our C isotopic results, we concluded that under drier conditions (e.g., Bokspits), shrubs would become an important source of SOC, whereas under wetter conditions (Shakawe), trees would become a significant source of SOC. Grasses, on the other hand, become an important source of SOC under optimal climate conditions (intermediate sites). Furthermore, changes in species composition and structure would affect N cycling in savanna ecosystems. For instance, as shrubs and thickets dominated the drier landscapes, most of the plants required N will be derived from the atmosphere through the process of N fixation. It is likely that under drier conditions, microbial activities would decrease, leading to a decrease in the nitrification process and ultimately resulting in very low quantities of plant-available N.

5. Conclusions

This field-based study aimed to shed light on how climate change would affect soil C sequestration in the savannas. Here, we used the Kalahari as a representative of global savannas. The steep precipitation gradient with homogeneous soil texture provided an environment conducive to decouple climatic effect from biogeophysical factors such as relief and soil texture. Our findings strongly indicate that belowground tree–grass interactions, and soil C sequestration in savannas are more complex than we thought and warrant a detailed soil C and N isotopic analysis. The soil profile of $\delta^{13}\text{C}$ and $\delta^{15}\text{N}$ is quite a lot more complex than simply representing root activity of C₃ and C₄ plants at depth. The co-existence of trees and grasses in savannas may be maintained by a vertical differentiation of root functional groups [109], contrary to the commonly assumed separated two-layer root system Walter [122]. However, this is outside the scope of this research.

We found that C₃ plants play an important role in SOC sequestration in the driest and wettest parts of the Kalahari. However, a detailed analysis revealed that in the driest part, shrubs contributed significantly to SOC, whereas in the wettest site, trees played

a significant role. C₄-dominated SOC sequestration in the intermediate sites. At these intermediate sites, we speculate that lower overall precipitation (than in the north) reduces the growth of trees, thus allowing water to penetrate deeper into the soil to reach the intermediate-depth grass roots. The result of this would be the production of more grass roots biomass, which translates into high C sequestration.

Using the Kalahari transect as a space-for-time substitution to assess the impact of climate change on soil C sequestration, we conclude that under extreme dry conditions, grasses and shrubs would become an important component of C sequestration. Conversely, under wetter conditions, trees would contribute significantly to soil C. Under moderate climate conditions, grasses have a competitive advantage over trees, and as a result, grasses would become an important source of soil C. It is, however, critical to acknowledge that our study covered only four sites along a 1000 km transect. Because savannas are found on all the continents, save for Antarctica, more detailed and intensive studies are needed to fully understand the potential impact of climate change on carbon cycling in savannas.

Supplementary Materials: The following supporting information can be downloaded at: <https://www.mdpi.com/article/10.3390/land14122328/s1>. Table S1: Soil $\delta^{13}\text{C}$ and tree-grass C input. The wettest site had the lowest soil $\delta^{13}\text{C}$ values. Soil $\delta^{13}\text{C}$ values were highest at 30 cm depth in all the sites. The standard errors are for multiple-sample analysis; Table S2: Soil and tree $\delta^{15}\text{N}$. The wettest site had the lowest soil $\delta^{15}\text{N}$ values. The difference between plant $\delta^{15}\text{N}$ and soil $\delta^{15}\text{N}$ was lowest in the second wettest site and highest in the second driest site. The standard errors are for multiple-sample analysis.

Author Contributions: Conceptualization, G.S.O. and P.D.; methodology, G.S.O. and P.D.; formal analysis, K.D., G.S.O. and P.D.; investigation, K.D., G.S.O., P.D., F.O., W.P.G.III, A.B., M.T. and L.W.; writing—original draft preparation, K.D., G.S.O., P.D., F.O., A.B. and L.W.; writing—review and editing, K.D., G.S.O., P.D., F.O., W.P.G.III, A.B., M.T. and L.W.; funding acquisition, G.S.O. and P.D. All authors have read and agreed to the published version of the manuscript.

Funding: This research was funded by NSF grants DEB-0717448 and EAR-1148334, NASA grants NNX11AQ16G and 80NSSC24K0298, the Princeton Environmental Institute internship program, and the UCLA Graduate Division Dissertation Year Fellowship.

Data Availability Statement: The original contributions presented in this study are included in the article/supplementary material. Further inquiries can be directed to the corresponding authors.

Acknowledgments: The data presented in this manuscript were derived from the Ph.D. thesis (Chapter 2) of K.D. We thank T. Harst, D. Perrot, M. Lu, M. O'Connor, C. Bonthuis, M. Patterson, D. Rachal, T. Meyer, D. Chavarro Rincon, R. Wellbeloved-Stone, H. Riffel, M. McDonald, O. Mathata, U. Mathata, M. Fischella and K. Kaseke for their great contributions to field and laboratory work. We also thank Martin for allowing us to work on his ranch. We also greatly thank the Departments of Forestry and Range Resources and Meteorological Services in Botswana for their invaluable contribution during the field campaign and provision of climate data, respectively. Lastly, we would like to thank the Ministry of Environment, Wildlife and Tourism, Botswana, for granting us a research permit: EWT 8/36/4 II (46). The authors have reviewed and edited the output and take full responsibility for the content of this publication.

Conflicts of Interest: The authors declare no conflicts of interest. The funders had no role in the design of the study; in the collection, analyses, or interpretation of data; in the writing of the manuscript; or in the decision to publish the results.

References

1. Scholes, R.J.; Archer, S.R. Tree-Grass interactions in savannas. *Annu. Rev. Ecol. Syst.* **1997**, *28*, 517–544. [[CrossRef](#)]
2. Sankaran, M.; Hanan, N.P.; Scholes, R.J.; Ratnam, J.; Augustine, D.J.; Cade, B.S.; Gignoux, J.; Higgins, S.I.; Le Roux, X.; Ludwig, F.; et al. Determinants of woody cover in African savannas. *Nature* **2005**, *438*, 846–849. [[CrossRef](#)] [[PubMed](#)]

3. Grunow, J.O.; Groeneveld, H.T.; Toit, S.H.C.D. Above-Ground Dry Matter Dynamics of the Grass Layer of a South African Tree Savanna. *J. Ecol.* **1980**, *68*, 877–889. [[CrossRef](#)]
4. Belsky, A.J. Influences of Trees on Savanna Productivity: Tests of Shade, Nutrients, and Tree-Grass Competition. *Ecology* **1994**, *75*, 922–932. [[CrossRef](#)]
5. Bond, W.J.; Parr, C.L. Beyond the forest edge: Ecology, diversity and conservation of the grassy biomes. *Biol. Conserv.* **2010**, *143*, 2395–2404. [[CrossRef](#)]
6. Grubb, P.J. The Maintenance of Species-Richness in Plant Communities: The Importance of the Regeneration Niche. *Biol. Rev.* **1977**, *52*, 107–145. [[CrossRef](#)]
7. Walker, B.H.; Noy-Meir, I. Aspects of the Stability and Resilience of Savanna Ecosystems. In *Ecology of Tropical Savannas*; Huntley, B.J., Walker, B.H., Eds.; Springer: Berlin/Heidelberg, Germany, 1982; pp. 556–590.
8. Bate, G.C.; Furniss, P.R.; Pendle, B.G. Water Relations of Southern African Savannas. In *Ecology of Tropical Savannas*; Huntley, B.J., Walker, B.H., Eds.; Springer: Berlin/Heidelberg, Germany, 1982; pp. 336–358.
9. Hipondoka, M.H.T.; Aranibar, J.N.; Chirara, C.; Lihavha, M.; Macko, S.A. Vertical distribution of grass and tree roots in arid ecosystems of Southern Africa: Niche differentiation or competition? *J. Arid Environ.* **2003**, *54*, 319–325. [[CrossRef](#)]
10. Shmida, A.; Ellner, S. Coexistence of plant species with similar niches. *Vegetatio* **1984**, *58*, 29–55. [[CrossRef](#)]
11. Glenn, E.; Squires, V.; Olsen, M.; Frye, R. Potential for carbon sequestration in the drylands. *Water Air Soil Pollut.* **1993**, *70*, 341–355. [[CrossRef](#)]
12. Jobbágy, E.G.; Jackson, R.B. The vertical distribution of soil organic carbon and its relation to climate and vegetation. *Ecol. Appl.* **2000**, *10*, 423–436. [[CrossRef](#)]
13. Grace, J.; José, J.S.; Meir, P.; Miranda, H.S.; Montes, R.A. Productivity and carbon fluxes of tropical savannas. *J. Biogeogr.* **2006**, *33*, 387–400. [[CrossRef](#)]
14. Dintwe, K.; Okin, G.S.; D’Odorico, P.; Hrast, T.; Mladenov, N.; Handorean, A.; Bhattachan, A.; Caylor, K.K. Soil organic C and total N pools in the Kalahari: Potential impacts of climate change on C sequestration in savannas. *Plant Soil* **2014**, *396*, 27–44. [[CrossRef](#)]
15. White II, D.A.; Welty-Bernard, A.; Rasmussen, C.; Schwartz, E. Vegetation controls on soil organic carbon dynamics in an arid, hyperthermic ecosystem. *Geoderma* **2009**, *150*, 214–223. [[CrossRef](#)]
16. Nicholson, S.E.; Kim, J. The relationship of the El Niño-Southern Oscillation to African rainfall. *Int. J. Climatol.* **1997**, *17*, 117–135. [[CrossRef](#)]
17. Nicholson, S.E. Climatic and environmental change in Africa during the last two centuries. *Clim. Res.* **2001**, *17*, 123–144. [[CrossRef](#)]
18. Knapp, A.K.; Beier, C.; Briske, D.D.; Classen, A.T.; Luo, Y.; Reichstein, M.; Smith, M.D.; Smith, S.D.; Bell, J.E.; Fay, P.A.; et al. Consequences of More Extreme Precipitation Regimes for Terrestrial Ecosystems. *BioScience* **2008**, *58*, 811–821. [[CrossRef](#)]
19. Shongwe, M.E.; van Oldenborgh, G.J.; van den Hurk, B.J.J.M.; de Boer, B.; Coelho, C.A.S.; van Aalst, M.K. Projected Changes in Mean and Extreme Precipitation in Africa under Global Warming. Part I: Southern Africa. *J. Clim.* **2009**, *22*, 3819–3837. [[CrossRef](#)]
20. IPCC. *Climate Change 2013: The Physical Science Basis. Working Group I Contribution to the IPCC 5th Assessment Report*; IPCC Secretariat: Geneva, Switzerland, 2013.
21. Batisani, N.; Yarnal, B. Rainfall variability and trends in semi-arid Botswana: Implications for climate change adaptation policy. *Appl. Geogr.* **2010**, *30*, 483–489. [[CrossRef](#)]
22. Dintwe, K.; Okin, G.S. Soil organic carbon in savannas decreases with anthropogenic climate change. *Geoderma* **2018**, *309*, 7–16. [[CrossRef](#)]
23. Cao, M.; Zhang, Q.; Shugart, H.H. Dynamic responses of African ecosystem carbon cycling to climate change. *Clim. Res.* **2001**, *17*, 183–193. [[CrossRef](#)]
24. Schlesinger, W.H.; Reynolds, J.F.; Cunningham, G.L.; Huenneke, L.F.; Jarrell, W.M.; Virginia, R.A.; Whitford, W.G. Biological Feedbacks in Global Desertification. *Science* **1990**, *247*, 1043–1048. [[CrossRef](#)]
25. Zeng, N.; Neelin, J.D. The Role of Vegetation–Climate Interaction and Interannual Variability in Shaping the African Savanna. *J. Clim.* **2000**, *13*, 2665–2670. [[CrossRef](#)]
26. Grace, P.R.; Post, W.M.; Hennessy, K. The potential impact of climate change on Australia’s soil organic carbon resources. *Carbon Balance Manag.* **2006**, *1*, 14. [[CrossRef](#)] [[PubMed](#)]
27. Gray, J.; Bishop, T. Mapping change in key soil properties due to climate change over south-eastern Australia. *Soil Res.* **2019**, *57*, 467–481. [[CrossRef](#)]
28. Ayarza, M.; Rao, I.; Vilela, L.; Lascano, C.; Vera, R. Soil carbon accumulation in crop–livestock systems in acid soil savannas of South America: A review. In *Advances in Agronomy*; Academic Press: Cambridge, MA, USA, 2022.
29. Castellano, G.R.; Santos, L.A.; Menegário, A.A. Carbon Soil Storage and Technologies to Increase Soil Carbon Stocks in the South American Savanna. *Sustainability* **2022**, *14*, 5571. [[CrossRef](#)]

30. Locatelli, J.L.; Grosso, S.D.; Santos, R.S.; Hong, M.; Gurung, R.; Stewart, C.E.; Cherubin, M.R.; Bayer, C.; Cerri, C.E.P. Modeling soil organic matter changes under crop diversification strategies and climate change scenarios in the Brazilian Cerrado. *Agric. Ecosyst. Environ.* **2025**, *379*, 109334. [[CrossRef](#)]
31. Rittl, T.F.; Oliveira, D.; Cerri, C.E.P. Soil carbon stock changes under different land uses in the Amazon. *Geoderma Reg.* **2017**, *10*, 138–143. [[CrossRef](#)]
32. Wei, X.; Shao, M.; Gale, W.; Li, L. Global pattern of soil carbon losses due to the conversion of forests to agricultural land. *Sci. Rep.* **2014**, *4*, 4062. [[CrossRef](#)] [[PubMed](#)]
33. Smith, N.G.; Schuster, M.J.; Dukes, J.S. Rainfall variability and nitrogen addition synergistically reduce plant diversity in a restored tallgrass prairie. *J. Appl. Ecol.* **2016**, *53*, 579–586. [[CrossRef](#)]
34. Huang, J.; Wu, P.; Zhao, X. Effects of rainfall intensity, underlying surface and slope gradient on soil infiltration under simulated rainfall experiments. *Catena* **2013**, *104*, 93–102. [[CrossRef](#)]
35. Thomas, B.F.; Behrangi, A.; Famiglietti, J.S. Precipitation Intensity Effects on Groundwater Recharge in the Southwestern United States. *Water* **2016**, *8*, 90. [[CrossRef](#)]
36. Jin, Y.; Goulden, M.L. Ecological consequences of variation in precipitation: Separating short-versus long-term effects using satellite data: Ecological effects of precipitation variation. *Glob. Ecol. Biogeogr.* **2014**, *23*, 358–370. [[CrossRef](#)]
37. Berry, R.S.; Kulmatiski, A. A savanna response to precipitation intensity. *PLoS ONE* **2017**, *12*, e0175402. [[CrossRef](#)] [[PubMed](#)]
38. Colwell, R.K.; Brehm, G.; Cardelús, C.L.; Gilman, A.C.; Longino, J.T. Global Warming, Elevational Range Shifts, and Lowland Biotic Attrition in the Wet Tropics. *Science* **2008**, *322*, 258–261. [[CrossRef](#)]
39. Bombelli, A.; Henry, M.; Castaldi, S.; Adu-Bredu, S.; Arneeth, A.; de Grandcourt, A.; Grieco, E.; Kutsch, W.L.; Lehsten, V.; Rasile, A.; et al. An outlook on the Sub-Saharan Africa carbon balance RID A-7494-2011 RID D-1226-2010. *Biogeosciences* **2009**, *6*, 2193–2205. [[CrossRef](#)]
40. Ciais, P.; Bombelli, A.; Williams, M.; Piao, S.L.; Chave, J.; Ryan, C.M.; Henry, M.; Brender, P.; Valentini, R. The Carbon Balance of Africa: Synthesis of Recent Research Studies. *Philos. Trans. R. Soc. A* **2011**, *369*, 2038–2057. [[CrossRef](#)]
41. Ries, L.P.; Shugart, H.H. Nutrient limitations on understory grass productivity and carbon assimilation in an African woodland savanna. *J. Arid Environ.* **2008**, *72*, 1423–1430. [[CrossRef](#)]
42. Bai, E.; Boutton, T.W.; Liu, F.; Wu, X.B.; Hallmark, C.T.; Archer, S.R. Spatial variation of soil $\delta^{13}\text{C}$ and its relation to carbon input and soil texture in a subtropical lowland woodland. *Soil Biol. Biochem.* **2012**, *44*, 102–112. [[CrossRef](#)]
43. Zhou, Y.; Mushinski, R.; Hyodo, A.; Wu, X.; Boutton, T. Vegetation change alters soil profile $\delta^{15}\text{N}$ values at the landscape scale. *Soil Biol. Biochem.* **2018**, *119*, 110–120. [[CrossRef](#)]
44. West, J.B.; Bowen, G.J.; Cerling, T.E.; Ehleringer, J.R. Stable isotopes as one of nature's ecological recorders. *Trends Ecol. Evol.* **2006**, *21*, 408–414. [[CrossRef](#)]
45. Ehleringer, J.R.; Buchmann, N.; Flanagan, L.B. Carbon Isotope Ratios in Belowground Carbon Cycle Processes. *Ecol. Appl.* **2000**, *10*, 412–422. [[CrossRef](#)]
46. Boutton, T.W.; Archer, S.R.; Midwood, A.J.; Zitzer, S.F.; Bol, R. $\delta^{13}\text{C}$ values of soil organic carbon and their use in documenting vegetation change in a subtropical savanna ecosystem. *Geoderma* **1998**, *82*, 5–41. [[CrossRef](#)]
47. Wang, L.; D'Odorico, P.; Ries, L.; Macko, S.A. Patterns and implications of plant-soil $\delta^{13}\text{C}$ and $\delta^{15}\text{N}$ values in African savanna ecosystems. *Quat. Res.* **2010**, *73*, 77–83. [[CrossRef](#)]
48. Ringrose, S.; Matheson, W.; Wolski, P.; Huntsman-Mapila, P. Vegetation cover trends along the Botswana Kalahari transect. *J. Arid Environ.* **2003**, *54*, 297–317. [[CrossRef](#)]
49. Bird, M.I.; Veenendaal, E.M.; Lloyd, J.J. Soil carbon inventories and $\delta^{13}\text{C}$ along a moisture gradient in Botswana. *Glob. Change Biol.* **2004**, *10*, 342–349. [[CrossRef](#)]
50. Tyson, P.D.; Crimp, S.J. The Climate of the Kalahari Transect. *Trans. R. Soc. S. Afr.* **1998**, *53*, 93–112. [[CrossRef](#)]
51. Thomas, A.D.; Shaw, P.A. *The Kalahari Environment*; Cambridge University Press: Cambridge, UK, 1991.
52. Hulme, M. *Climate Change and Southern Africa: An Exploration of Some Potential Impacts and Implications in the SADC (Southern African Development Community) Region*; Climatic Research Unit, University of East Anglia, World Wide Fund for Nature: Norwich, UK, 1996.
53. Shugart, H.H.; Macko, S.A.; Lesolle, P.; Szuba, T.A.; Mukelabai, M.M.; Dowty, P.; Swap, R.J. The SAFARI 2000—Kalahari Transect Wet Season Campaign of year 2000. *Glob. Change Biol.* **2004**, *10*, 273–280. [[CrossRef](#)]
54. Scholes, R.J.; Dowty, P.R.; Caylor, K.; Parsons, D.A.B.; Frost, P.G.H.; Shugart, H.H. Trends in Savanna Structure and Composition along an Aridity Gradient in the Kalahari. *J. Veg. Sci.* **2002**, *13*, 419–428. [[CrossRef](#)]
55. Wang, L.; D'Odorico, P.; Ringrose, S.; Coetzee, S.; Macko, S.A. Biogeochemistry of Kalahari sands. *J. Arid Environ.* **2007**, *71*, 259–279. [[CrossRef](#)]
56. de Vries, J.J.; Selaolo, E.T.; Beekman, H.E. Groundwater recharge in the Kalahari, with reference to paleo-hydrologic conditions. *J. Hydrol.* **2000**, *238*, 110–123. [[CrossRef](#)]

57. Swap, R.J.; Aranibar, J.N.; Dowty, P.R.; Gilhooly Iii, W.P.; Macko, S.A. Natural abundance of ^{13}C and ^{15}N in C3 and C4 vegetation of southern Africa: Patterns and implications. *Glob. Change Biol.* **2004**, *10*, 350–358. [[CrossRef](#)]
58. Aranibar, J.N.; Otter, L.; Macko, S.A.; Feral, C.J.W.; Epstein, H.E.; Dowty, P.R.; Eckardt, F.; Shugart, H.H.; Swap, R.J. Nitrogen cycling in the soil–plant system along a precipitation gradient in the Kalahari sands. *Glob. Change Biol.* **2004**, *10*, 359–373. [[CrossRef](#)]
59. Caylor, K.K.; Shugart, H.H.; Dowty, P.R.; Smith, T.M. Tree spacing along the Kalahari transect in southern Africa. *J. Arid Environ.* **2003**, *54*, 281–296. [[CrossRef](#)]
60. Okin, G.S.; Mladenov, N.; Wang, L.; Cassel, D.; Caylor, K.K.; Ringrose, S.; Macko, S.A. Spatial patterns of soil nutrients in two southern African savannas. *J. Geophys. Res.* **2008**, *113*. [[CrossRef](#)]
61. Meyer, T.; D’Odorico, P.; Okin, G.S.; Shugart, H.H.; Caylor, K.K.; O’Donnell, F.C.; Bhattachan, A.; Dintwe, K. An analysis of structure: Biomass structure relationships for characteristic species of the western Kalahari, Botswana. *Afr. J. Ecol.* **2013**, *52*, 20–29. [[CrossRef](#)]
62. Bhattachan, A.; D’Odorico, P.; Dintwe, K.; Okin, G.S.; Collins, S.L. Resilience and recovery potential of duneland vegetation in the southern Kalahari. *Ecosphere* **2014**, *5*, 1–14. [[CrossRef](#)]
63. Bhattachan, A.; D’Odorico, P.; Okin, G.S.; Dintwe, K. Potential dust emissions from the southern Kalahari’s dunelands. *J. Geophys. Res. Earth Surf.* **2013**, *118*, 307–314. [[CrossRef](#)]
64. Koch, G.W.; Vitousek, P.M.; Steffen, W.L.; Walker, B.H. Terrestrial transects for global change research. *Plant Ecol.* **1995**, *121*, 53–65. [[CrossRef](#)]
65. Wang, L.; D’Odorico, P.; Okin, G.S.; Macko, S.A. Isotope composition and anion chemistry of soil profiles along the Kalahari Transect. *J. Arid Environ.* **2008**, *73*, 480–486. [[CrossRef](#)]
66. Bird, B.W.; Kirby, M.E.; Howat, I.M.; Tulaczyk, S. Geophysical evidence for Holocene lake-level change in southern California (Dry Lake). *Boreas* **2010**, *39*, 131–144. [[CrossRef](#)]
67. Kirby, M.E.; Knell, E.J.; Anderson, W.T.; Lachniet, M.S.; Palermo, J.; Eeg, H.; Lucero, R.; Murrieta, R.; Arevalo, A.; Silveira, E.; et al. Evidence for insolation and Pacific forcing of late glacial through Holocene climate in the Central Mojave Desert (Silver Lake, CA). *Quat. Res.* **2015**, *84*, 174–186. [[CrossRef](#)]
68. Harris, D.; Horwath, W.R.; van Kessel, C. Acid fumigation of soils to remove carbonates prior to total organic carbon or carbon-13 isotopic analysis. *Soil Sci. Soc. Am. J.* **2001**, *65*, 1853–1856. [[CrossRef](#)]
69. Olsson, I.U. *Radiocarbon Variations and Absolute Chronology; Proceedings*; Wiley Interscience Division, John Wiley & Sons: New York, NY, USA, 1970.
70. Craig, H. The geochemistry of the stable carbon isotopes. *Geochim. Cosmochim. Acta* **1953**, *3*, 53–92. [[CrossRef](#)]
71. Craig, H. Isotopic standards for carbon and oxygen and correction factors for mass-spectrometric analysis of carbon dioxide. *Geochim. Cosmochim. Acta* **1957**, *12*, 133–149. [[CrossRef](#)]
72. Amundson, R.; Stern, L.; Baisden, T.; Wang, Y. The isotopic composition of soil and soil-respired CO_2 . *Geoderma* **1998**, *82*, 83–114. [[CrossRef](#)]
73. Stuiver, M.; Polach, H.A. Reporting of ^{14}C Data. *Radiocarbon* **1977**, *19*, 355–363. [[CrossRef](#)]
74. Epstein, M.S.; Diamondstone, B.I.; Gills, T.E.; Adams, J.R. A New River Sediment Standard, Reference Material. *J. Res. Natl. Bur. Stand.* **1988**, *93*, 234. [[CrossRef](#)]
75. Peterson, B.J.; Fry, B. Stable Isotopes in Ecosystem Studies. *Annu. Rev. Ecol. Syst.* **1987**, *18*, 293–320. [[CrossRef](#)]
76. Mariotti, A. Atmospheric nitrogen is a reliable standard for natural ^{15}N abundance measurements. *Nature* **1983**, *303*, 685–687. [[CrossRef](#)]
77. O’Leary, M.H. Carbon Isotopes in Photosynthesis. *BioScience* **1988**, *38*, 328–336. [[CrossRef](#)]
78. O’Leary, M.H. Carbon isotope fractionation in plants. *Phytochemistry* **1981**, *20*, 553–567. [[CrossRef](#)]
79. Farquhar, G.D.; Ehleringer, J.R.; Hubick, K.T. Carbon Isotope Discrimination and Photosynthesis. *Annu. Rev. Plant Physiol. Plant Mol. Biol.* **1989**, *40*, 503–537. [[CrossRef](#)]
80. Keeling, C.D.; Piper, S.C.; Bacastow, R.B.; Wahlen, M.; Whorf, T.P.; Heimann, M.; Meijer, H.A. Atmospheric CO_2 and $^{13}\text{CO}_2$ Exchange with the Terrestrial Biosphere and Oceans from 1978 to 2000: Observations and Carbon Cycle Implications. In *A History of Atmospheric CO_2 and Its Effects on Plants, Animals, and Ecosystems*; Baldwin, I.T., Caldwell, M.M., Heldmaier, G., Jackson, R.B., Lange, O.L., Mooney, H.A., Schulze, E.D., Sommer, U., Ehleringer, J.R., Dearing, M.D., Eds.; Springer: New York, NY, USA, 2005; pp. 83–113.
81. Werner, R.A.; Brand, W.A. Referencing strategies and techniques in stable isotope ratio analysis. *Rapid Commun. Mass Spectrom.* **2001**, *15*, 501–519. [[CrossRef](#)] [[PubMed](#)]
82. Craine, J.M.; Brookshire, E.N.J.; Cramer, M.D.; Hasselquist, N.J.; Koba, K.; Marin-Spiotta, E.; Wang, L. Ecological interpretations of nitrogen isotope ratios of terrestrial plants and soils. *Plant Soil* **2015**, *396*, 1–26. [[CrossRef](#)]
83. Handley, L.L.; Raven, J.A. The use of natural abundance of nitrogen isotopes in plant physiology and ecology. *Plant Cell Environ.* **1992**, *15*, 965–985. [[CrossRef](#)]

84. Hobbie, E.A.; Macko, S.A.; Shugart, H.H. Interpretation of nitrogen isotope signatures using the NIFTE model. *Oecologia* **1999**, *120*, 405–415. [[CrossRef](#)]
85. Amundson, R.; Austin, A.T.; Schuur, E.a.G.; Yoo, K.; Matzek, V.; Kendall, C.; Uebersax, A.; Brenner, D.; Baisden, W.T. Global patterns of the isotopic composition of soil and plant nitrogen. *Glob. Biogeochem. Cycles* **2003**, *17*, 1031. [[CrossRef](#)]
86. Craine, J.M.; Elmore, A.J.; Wang, L.; Augusto, L.; Baisden, W.T.; Brookshire, E.N.J.; Cramer, M.D.; Hasselquist, N.J.; Hobbie, E.A.; Kahmen, A.; et al. Convergence of soil nitrogen isotopes across global climate gradients. *Sci. Rep.* **2015**, *5*, 8280. [[CrossRef](#)]
87. Shearer, G.; Kohl, D.H.; Virginia, R.A.; Bryan, B.A.; Skeeters, J.L.; Nilsen, E.T.; Sharifi, M.R.; Rundel, P.W. Estimates of N₂-fixation from variation in the natural abundance of ¹⁵N in Sonoran desert ecosystems. *Oecologia* **1983**, *56*, 365–373. [[CrossRef](#)]
88. Virginia, R.A.; Jarrell, W.M.; Rundel, P.W.; Shearer, G.; Kohl, D.H. The Use of Variation in the Natural Abundance of ¹⁵N to Assess Symbiotic Nitrogen Fixation by Woody Plants. In *Stable Isotopes in Ecological Research*; Rundel, P.W., Ehleringer, J.R., Nagy, K.A., Eds.; Springer: New York, NY, USA, 1989; pp. 375–394.
89. Dawson, T.E.; Mambelli, S.; Plamboeck, A.H.; Templer, P.H.; Tu, K.P. Stable Isotopes in Plant Ecology. *Annu. Rev. Ecol. Syst.* **2002**, *33*, 507–559. [[CrossRef](#)]
90. Phillips, D.L.; Gregg, J.W. Source partitioning using stable isotopes: Coping with too many sources. *Oecologia* **2003**, *136*, 261–269. [[CrossRef](#)] [[PubMed](#)]
91. Phillips, D.L.; Newsome, S.D.; Gregg, J.W. Combining sources in stable isotope mixing models: Alternative methods. *Oecologia* **2005**, *144*, 520–527. [[CrossRef](#)]
92. Setshogo, M.P.; Venter, F. *Trees of Botswana: Names and Distribution*; Southern African Botanical Diversity Network (SABONET): Pretoria, South Africa, 2003; p. 170.
93. Bird, M.I.; Pousai, P. Variations of $\delta^{13}\text{C}$ in the surface soil organic carbon pool. *Glob. Biogeochem. Cycles* **1997**, *11*, 313–322. [[CrossRef](#)]
94. Weiguo, L.; Xiahong, F.; Youfeng, N.; Qingle, Z.; Yunning, C.; Zhisheng, A.N. $\delta^{13}\text{C}$ variation of C₃ and C₄ plants across an Asian monsoon rainfall gradient in arid northwestern China. *Glob. Change Biol.* **2005**, *11*, 1094–1100. [[CrossRef](#)]
95. Sanaiotti, T.M.; Martinelli, L.A.; Victoria, R.L.; Trumbore, S.E.; Camargo, P.B. Past Vegetation Changes in Amazon Savannas Determined Using Carbon Isotopes of Soil Organic Matter. *Biotropica* **2002**, *34*, 2–16. [[CrossRef](#)]
96. Wang, L.; Okin, G.S.; Caylor, K.K.; Macko, S.A. Spatial heterogeneity and sources of soil carbon in southern African savannas. *Geoderma* **2009**, *149*, 402–408. [[CrossRef](#)]
97. Amundson, R. The Use of Stable Isotopes in Assessing the Effect of Agriculture on Arid and Semi-Arid Soils. In *Stable Isotopes in Ecological Research*; Rundel, P.W., Ehleringer, J.R., Nagy, K.A., Eds.; Springer: New York, NY, USA, 1989; pp. 318–341.
98. Ma, J.-Y.; Sun, W.; Liu, X.-N.; Chen, F.-H. Variation in the Stable Carbon and Nitrogen Isotope Composition of Plants and Soil along a Precipitation Gradient in Northern China. *PLoS ONE* **2012**, *7*, e51894. [[CrossRef](#)]
99. Dougill, A.J.; Thomas, A.D. Kalahari sand soils: Spatial heterogeneity, biological soil crusts and land degradation. *Land Degrad. Dev.* **2004**, *15*, 233–242. [[CrossRef](#)]
100. Bhattachan, A.; Tatlhego, M.; Dintwe, K.; O'Donnell, F.; Caylor, K.K.; Okin, G.S.; Perrot, D.O.; Ringrose, S.; D'Odorico, P. Evaluating Ecohydrological Theories of Woody Root Distribution in the Kalahari. *PLoS ONE* **2012**, *7*, e33996. [[CrossRef](#)]
101. Walker, B.; Langridge, J. Predicting savanna vegetation structure on the basis of plant available moisture (PAM) and plant available nutrients (PAN): A case study from Australia. *J. Biogeogr.* **1997**, *24*, 813–825. [[CrossRef](#)]
102. Gillson, L. Evidence of a tipping point in a southern African savanna? *Ecol. Complex.* **2015**, *21*, 78–86. [[CrossRef](#)]
103. Wynn, J.G.; Bird, M.I.; Wong, V.N.L. Rayleigh distillation and the depth profile of ¹³C/¹²C ratios of soil organic carbon from soils of disparate texture in Iron Range National Park, Far North Queensland, Australia. *Geochim. Cosmochim. Acta* **2005**, *69*, 1961–1973. [[CrossRef](#)]
104. Mordelet, P.; Menaut, J.-C.; Mariotti, A. Tree and Grass Rooting Patterns in an African Humid Savanna. *J. Veg. Sci.* **1997**, *8*, 65–70. [[CrossRef](#)]
105. February, E.C.; Higgins, S.I. The distribution of tree and grass roots in savannas in relation to soil nitrogen and water. *S. Afr. J. Bot.* **2010**, *76*, 517–523. [[CrossRef](#)]
106. February, E.C.; Cook, G.D.; Richards, A.E. Root dynamics influence tree–grass coexistence in an Australian savanna. *Austral Ecol.* **2013**, *38*, 66–75. [[CrossRef](#)]
107. Nilsen, E.T.; Sharifi, M.R.; Rundel, P.W.; Jarrell, W.M.; Virginia, R.A. Diurnal and Seasonal Water Relations of the Desert Phreatophyte *Prosopis Glandulosa* (Honey Mesquite) in the Sonoran Desert of California. *Ecology* **1983**, *64*, 1381–1393. [[CrossRef](#)]
108. Kambatuku, J.R.; Cramer, M.D.; Ward, D. Overlap in soil water sources of savanna woody seedlings and grasses. *Ecolhydrology* **2013**, *6*, 464–473. [[CrossRef](#)]
109. O'Donnell, F.C.; Caylor, K.K.; Bhattachan, A.; Dintwe, K.; D'Odorico, P.; Okin, G.S. A quantitative description of the interspecies diversity of belowground structure in savanna woody plants. *Ecosphere* **2015**, *6*, 1–15. [[CrossRef](#)]
110. Scanlon, T.M.; Albertson, J.D.; Caylor, K.K.; Williams, C.A. Determining land surface fractional cover from NDVI and rainfall time series for a savanna ecosystem. *Remote Sens. Environ.* **2002**, *82*, 376–388. [[CrossRef](#)]

111. Caylor, K.K.; D’Odorico, P.; Rodriguez-Iturbe, I. On the ecohydrology of structurally heterogeneous semiarid landscapes. *Water Resour. Res.* **2006**, *42*, 1–13. [[CrossRef](#)]
112. Ringrose, S.; Matheson, W.; Vanderpost, C. Analysis of soil organic carbon and vegetation cover trends along the Botswana Kalahari Transect. *J. Arid Environ.* **1998**, *38*, 379–396. [[CrossRef](#)]
113. Dohn, J.; Dembélé, F.; Karembé, M.; Moustakas, A.; Amévor, K.A.; Hanan, N.P. Tree effects on grass growth in savannas: Competition, facilitation and the stress-gradient hypothesis. *J. Ecol.* **2013**, *101*, 202–209. [[CrossRef](#)]
114. Ludwig, F.; Dawson, T.E.; Prins, H.H.T.; Berendse, F.; Kroon, H. Below-ground competition between trees and grasses may overwhelm the facilitative effects of hydraulic lift. *Ecol. Lett.* **2004**, *7*, 623–631. [[CrossRef](#)]
115. Ludwig, F.; de Kroon, H.; Berendse, F.; Prins, H.H.T. The influence of savanna trees on nutrient, water and light availability and the understorey vegetation. *Plant Ecol.* **2004**, *170*, 93–105. [[CrossRef](#)]
116. Priyadarshini, K.V.R.; Prins, H.H.T.; Bie, S.d.; Heitkönig, I.M.A.; Woodborne, S.; Gort, G.; Kirkman, K.; Fry, B.; Kroon, H.d. Overlap in nitrogen sources and redistribution of nitrogen between trees and grasses in a semi-arid savanna. *Oecologia* **2013**, *174*, 1107–1116. [[CrossRef](#)]
117. Hartmann, D.L.; Klein Tank, A.M.G.; Rusticucci, M.; Alexander, L.V.; Brönnimann, S.; Charabi, Y.; Dentener, F.J.; Dlugokencky, E.J.; Easterling, D.R.; Kaplan, A.; et al. Observations: Atmosphere and Surface. In *Climate Change 2013: The Physical Science Basis. Contribution of Working Group I to the Fifth Assessment Report of the Intergovernmental Panel on Climate Change*; Stocker, T.F., Qin, D., Plattner, G.K., Tignor, M., Allen, S.K., Boschung, J., Nauels, A., Xia, Y., Bex, V., Midgley, P.M., Eds.; Cambridge University Press: Cambridge, UK; New York, NY, USA, 2013; pp. 159–254.
118. Willis, K.J.; Bennett, K.D.; Burrough, S.L.; Macias-Fauria, M.; Tovar, C. Determining the response of African biota to climate change: Using the past to model the future. *Philos. Trans. R. Soc. B Biol. Sci.* **2013**, *368*, 20120491. [[CrossRef](#)]
119. Anadón, J.D.; Sala, O.E.; Maestre, F.T. Climate change will increase savannas at the expense of forests and treeless vegetation in tropical and subtropical Americas. *J. Ecol.* **2014**, *102*, 1363–1373. [[CrossRef](#)]
120. Higgins, S.I.; Scheiter, S. Atmospheric CO₂ forces abrupt vegetation shifts locally, but not globally. *Nature* **2012**, *488*, 209–212. [[CrossRef](#)] [[PubMed](#)]
121. Archer, S.; Schimel, D.S.; Holland, E.A. Mechanisms of shrubland expansion: Land use, climate or CO₂? *Clim. Change* **1995**, *29*, 91–99. [[CrossRef](#)]
122. Walter, H. *Vegetation of the Earth in Relation to Climate and the Eco-Physiological Conditions*, 1st ed.; Springer: London, UK; New York, NY, USA, 1973; p. 230.

Disclaimer/Publisher’s Note: The statements, opinions and data contained in all publications are solely those of the individual author(s) and contributor(s) and not of MDPI and/or the editor(s). MDPI and/or the editor(s) disclaim responsibility for any injury to people or property resulting from any ideas, methods, instructions or products referred to in the content.